CHEMISTRY OF MATERIALS

pubs.acs.org/cm Article

Understanding of Face-On Crystallites Transitioning to Edge-On Crystallites in Thiophene-Based Conjugated Polymers

Sung Yun Son, Taiho Park,* and Wei You*

Cite This: *Chem. Mater.* 2021, 33, 4541−4550 Read Online

ACCESS | Metrics & More | Article Recommendations | Supporting Information

ABSTRACT: The orientation of crystallites (face-on or edge-on, in regard to the plane of the substrate) in semicrystalline conjugated polymer thin films has a significant impact on charge transport properties of such thin films. It has been observed in a number of conjugated polymers where predominantly face-on orientation in the as-cast film can transition to edge-on upon cooling from the melt (melt-annealing). However, why and how do face-on crystallites transition to edge-on during melt-annealing remain unclear. To answer these fundamental questions, we designed and synthesized a random copolymer (RP-3T) by inserting unsubstituted terthiophenes into regioregular poly(3-hexylthiophene)s. RP-3T shows a predominantly face-on orientation in an as-cast film but transitioning to an almost exclusively edge-on orientation upon annealing at 190 °C, a temperature below the T_m (194 °C). Through a detailed investigation on changes in the microstructure and orientation of crystallites in RP-3T with annealing temperature, we find that face-on crystallites in RP-3T start to disappear at 170 °C (notably lower than the T_m), while edge-on crystallites continue to grow as the annealing temperature increases toward the T_m. This finding provides a reasonable explanation for the transition of face-on orientation to edge-on orientation during thermal annealing in RP-3T, in particular, at a temperature below the T_m.

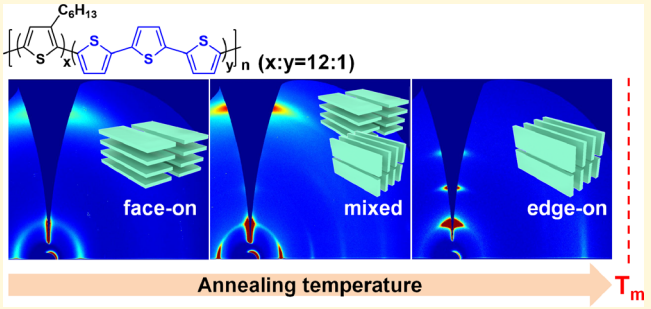

INTRODUCTION

Compared with inorganic semiconductors, organic semiconductors, particularly conjugated polymers (CPs), have distinctive advantages including light weight, tunable optoelectronic properties, and potential for roll-to-roll production on flexible substrates.[1−4] Indeed, CPs have been intensively investigated in the field of organic electronics including organic photovoltaics (OPVs)[5] and organic field-effect transistors (OFETs).[6] For both OFETs and OPVs, high mobilities of charge carriers are required to maximize the device performance. Thus, a significant amount of effort has been devoted to understanding the factors that would affect the charge transport in CPs, in particular, as thin films—the typical physical state of CPs in both OPVs and OFETs.[7−9]

Previous efforts have revealed that charge transport in CP-based thin films is significantly affected by several morphological parameters such as crystallinity, chain packing distances in crystalline domains, connectivity between crystalline domains via tie chains, and orientation of crystallites.[10] Among these, the orientation of crystallites is considered to have a significant impact on charge transport in a given direction (e.g., vertical vs horizontal to the substrate plane).[11] This is because in crystalline domains of CPs, intermolecular charge transport occurs along the $\pi-\pi$ stacking direction but is forbidden along the lamellar packing direction due to the insulating side chains.[12] Therefore, it is believed that a predominantly edge-on orientation of crystallites, where the $\pi-\pi$ stacking direction is parallel to the substrate plane, is advantageous for horizontal/lateral charge transport (e.g., in OFETs); in contrast, a predominantly face-on orientation, where the $\pi-\pi$ stacking direction is perpendicular to the substrate plane, is beneficial for vertical charge transport (e.g., in OPVs).[10]

The specific orientation (edge-on, face-on, or mixed) that CPs adopt on a substrate can be influenced by a number of factors, including intrinsic properties of CPs (e.g., chemical structure, molecular weight, degree of regioregularity, etc.) and extrinsic—often processing-related—factors (e.g., solvent, annealing, surface properties, etc.).[13] For example, the pioneering work by Sirringhaus et al. revealed that the orientation of crystallites in poly(3-hexylthiophene) (P3HT) can vary depending on the degree of regioregularity and the molecular weight of P3HT.[11] The authors observed that the regioregular P3HT with a low molecular weight showed a

Received: March 17, 2021
Revised: May 20, 2021
Published: June 7, 2021

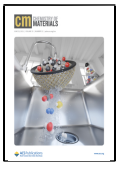

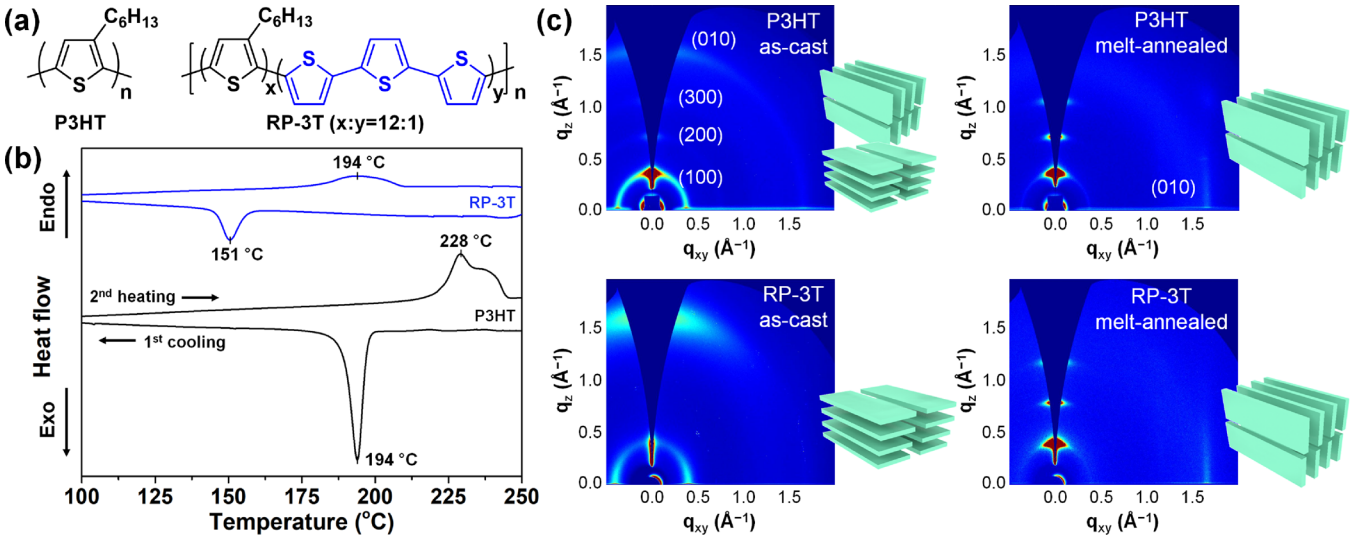

Figure 1. (a) Chemical structures and (b) DSC thermograms of P3HT and RP-3T. (c) GIWAXS patterns of as-cast and melt-annealed films of P3HT and RP-3T. The insets in (c) represent mixed, face-on, and edge-on orientations for the P3HT as-cast film, RP-3T as-cast film, and melt-annealed film of both polymers, respectively.

predominantly edge-on orientation, whereas the regioirregular P3HT with a high molecular weight displayed a predominantly face-on orientation.[11]

For the more prevalent donor−acceptor (D−A) polymers, it has been observed that alteration of donor moieties,[14,15] tailoring of backbone coplanarity,[16] and modulation of intramolecular noncovalent interactions[17,18] can result in a drastic change in the orientation of crystallites. Furthermore, varying the side chains of such CPs can also change the orientation of the crystallites.[19−21] Apart from these intrinsic properties of CPs, extrinsic factors such as solvent,[22,23] spin-coating speed,[24] film coating method,[25−27] and surface properties of the substrate[28−30] have been reported to have an impact on the crystallite orientation of CPs.

Interestingly, it has been found that the face-on or mixed orientation of crystallites in CP-based thin films can transition into the edge-on orientation upon annealing above the melting temperature (T_m) of the CP, followed by subsequent cooling (i.e., "melt-annealing"). In one example, Bao and co-workers reported that P3HT films, which had a mixed orientation upon solution casting, adopted a strong edge-on preferential orientation after melt-annealing.[31] In another example, Salleo and co-workers observed that poly{[*N*,*N*′-bis(2-octyldodecyl)-naphthalene-1,4,5,8-bis(dicarboximide)-2,6-diyl]-*alt*-5,5′-(2,2′-bithiophene)} (N2200) underwent a change in the predominant orientation from face-on to edge-on upon melt-annealing.[32] Moreover, similar behaviors (i.e., face-on to edge-on upon melt-annealing) have also been observed in other CPs[33−35] and even small molecules.[36] It was thought that such re-orientation possibly occurred due to heterogeneous nucleation of edge-on crystallites upon cooling from the melt,[31,32] yet why and how face-on crystallites transition to edge-on during melt-annealing have not been clearly understood. In the case of N2200, Brinkmann and co-workers showed two different polymorphs—different by the stacking mode of the naphthalenediimide and bithiophene units—could explain the face-on to edge-on transition upon thermal annealing,[29,37] yet the exact reason for the observed transition of the orientation direction was not clearly addressed.

To address these fundamental questions, one needs to identify and investigate CPs that would adopt a predominantly face-on orientation as spun (and then would transition to edge-on orientation upon melt-annealing). Although N2200 would be a good candidate per the study by Salleo and co-workers, we chose to focus on more representing thiophene-based CPs because thiophene-containing CPs are ubiquitous and there is a wealth of knowledge about morphologies of thiophene-based CPs.[7,11,38,39] In addition, polythiophenes can be synthesized via the Grignard metathesis (GRIM) polymerization that allows an excellent control of molecular parameters such as the degree of regioregularity[40] and molecular weight.[41,42] However, designing such special polythiophenes to achieve a predominantly face-on orientation is not straightforward. Searching for inspiration for molecular design, we noted an earlier work by Zhang et al. where the authors reported that the number of unsubstituted thiophene units between two diketopyrrolopyrrole (DPP) units played an important role in determining the crystallite orientation in DPP-based CPs.[14] Importantly, the authors suggested that a higher side chain density, enabled by using a smaller number of unsubstituted thiophene units in between the substituted DPP units, would hinder regular lamellar packing along the out-of-plane direction and lead to the π−face parallel to the substrate, i.e., face-on orientation.

Aiming to achieve polythiophenes adopting a face-on orientation as spun for our investigation, we introduced unsubstituted terthiophene (3T) units into P3HT in a random manner (RP-3T in Figure 1a), anticipating that the resulting random configuration would also disrupt regular lamellar packing perpendicular to the substrate, and consequently, the polymer chains would preferentially adopt a face-on orientation. For comparison, we also synthesized regioregular P3HT. Both polymers were synthesized to have similar degrees of regioregularity and molecular weights, to minimize the interference of such intrinsic properties of polymers in interpreting the observed difference in the orientations of crystallites between these two polymers.

Probing the initial texture and molecular packing of both polymers in as-cast films using grazing incidence wide-angle X-

https://doi.org/10.1021/acs.chemmater.1c00946
Chem. Mater. 2021, 33, 4541−4550

ray scattering (GIWAXS) (Figure 1c) indicated that RP-3T indeed showed a predominantly face-on orientation, whereas P3HT had the mixed orientation with the edge-on orientation being dominant. However, the initial orientation in both P3HT and RP-3T as-cast thin films transitioned to almost exclusively edge-on upon melt-annealing (Figure 1c). Given that RP-3T showed a stark difference in the orientation upon melt-annealing, i.e., from predominantly face-on to almost exclusively edge-on, RP-3T presented itself as an ideal system to carry out our proposed investigation. Through a systematic and detailed study (*vide infra*), we found that the re-orientation of crystallites occurred in RP-3T from the initial face-on orientation to the mixed orientation and finally to the edge-on orientation as the annealing temperature increased toward the T_m of RP-3T; in fact, face-on crystallites began to disappear at 170 °C, a temperature below the T_m of RP-3T, while edge-on crystallites continued to grow with an increased annealing temperature. Further data showed that edge-on and face-on crystallites have different packing distances, which presumably lead to more stable edge-on crystallites and therefore induce the re-orientation from face-on orientation to edge-on orientation.

RESULTS AND DISCUSSION

Synthesis and Characterization. P3HT and RP-3T were synthesized via GRIM polymerization (see details in the Supporting Information). Specifically, RP-3T was synthesized by copolymerizing the 3-hexylthiophene (3-HT) monomer with the 3T monomer. The monomer feed ratio for RP-3T was 12: 1 (3-HT:3T), aiming to have 20 mol % of unsubstituted thiophenes in the conjugated backbones of RP-3T since addition of ∼30 mol % of unsubstituted thiophenes could considerably lower the crystallinity of resulting polythiophenes.[43] The actual molar ratio of incorporated unsubstituted thiophene was 22.8 mol %, calculated from the integration of aromatic protons in the ^{1}H NMR spectra (Figure S1). This indicates that 3T monomers were well incorporated into the conjugated backbone of P3HT, likely in a random fashion. Importantly, the incorporation of 3T monomers does not seem to disturb the regioregularity of the conjugated backbone, according to the ^{1}H NMR spectra. The degrees of regioregularity for the synthesized P3HT and RP-3T were 96.2 and 97.1%, respectively (Table 1), determined by comparing the integration of α-methylene protons of the hexyl group of the head-to-tail configuration (2.70−2.85 ppm) and the head-to-head configuration (2.55−2.65 ppm) in the ^{1}H NMR spectrum (Figures S1 and S2).[44]

Table 1. Regioregularity, Molecular Weights, Dispersity, and Thermal Properties for P3HT and RP-3T

polymer	regioregularity (%)	M_n[a] ($Đ$)	T_c[b] (°C)	T_m[c] (°C)
P3HT	96.2	16,800 (1.07)	194	228
RP-3T	97.1	15,200 (1.38)	151	194

[a]Number-average molecular weights measured by GPC with chlorobenzene eluent using a calibration curve of polystyrene standards. [b]Crystallization temperature. [c]Melting temperature. T_c and T_m are the exothermic and endothermic peak temperatures, respectively, measured using DSC.

The molecular weights and dispersities of the polymers were determined by gel permeation chromatography (GPC) using polystyrene standards as calibrants. The two polymers have similar molecular weights (Table 1), eliminating the potential complication of having different molecular weights in interpreting morphology. We note that RP-3T has a higher dispersity than P3HT, which can be attributed to some premature termination of chain propagation due to the limited solubility-induced precipitation of some polymers when more than two 3T monomers were attached successively to the growing chain end.

To evaluate crystallinity, the polymers were investigated using differential scanning calorimetry (DSC). The T_m and crystallization temperature (T_c) are summarized in Table 1. P3HT shows distinct endothermic and exothermic peaks in the second heating and first cooling curves, corresponding to the melting and crystallization processes, respectively (Figure 1b). RP-3T has lower values of T_m and T_c, and the endothermic/exothermic peaks are much less distinct when compared to those of P3HT, indicating that RP-3T has a lower degree of crystallinity than P3HT, likely due to the random insertion of unsubstituted thiophenes.[45,46]

As-cast and melt-annealed films of the polymers were characterized using GIWAXS to study their initial morphologies and changes in the morphologies upon melt-annealing. As shown in Figure 1c, the GIWAXS pattern of as-cast P3HT shows out-of-plane (h00) and (010) peaks, corresponding to out-of-plane lamellar packing and $\pi-\pi$ stacking, respectively. This observation indicates a mixed orientation in the as-case film of P3HT. However, the melt-annealed film of P3HT shows a preferential edge-on orientation, which is very similar to what Bao et al. previously observed.[31] Surprisingly, the as-cast film of RP-3T shows a completely different GIWAXS pattern (Figure 1c), where strong out-of-plane (010) and in-plane (100) peaks appear, indicative of a preferential face-on orientation. Our earlier work indicates that the random insertion of unsubstituted monothiophene (1T) units into P3HT did not lead to a preferential face-on orientation;[43] hence, it may be inferred that 3T units, distributed randomly in the conjugated backbone of RP-3T, can more effectively hinder out-of-plane lamellar packing during fast film formation via spin-coating, and a face-on orientation would thus be preferentially achieved.[14] Interestingly, the melt-annealed film of RP-3T displays a completely different GIWAXS pattern: strong out-of-plane (h00) and in-plane (010) peaks, indicating an almost exclusively edge-on orientation (Figure 1c). This suggests that molten amorphous chains would crystallize into edge-on crystallites upon cooling from the melt as previously observed in other CPs.[31−35] Since the as-cast film of RP-3T showed a predominantly face-on orientation as spun and transitioned to an edge-on orientation after melt-annealing (Figure 1c), we chose RP-3T as the "model" polymer to further investigate the changes in microstructures and the orientation of crystallites in its thin film with the annealing temperature.

Investigating the Microstructure and Orientation of Crystallites with Annealing Temperature via GIWAXS. Experimentally, the RP-3T films (coated on a bare Si wafer via spin-coating) were annealed at a predetermined temperature (80−190 °C) for 10 min and cooled back to room temperature under an ambient condition and then characterized using GIWAXS (see the Experimental Section for the detailed film preparation condition). Compared to the as-cast film, the intensity of all peaks becomes stronger when the RP-3T film was annealed at 80 °C (Figure 2a). As the annealing temperature increases, for example, at 110 °C, the annealed

https://doi.org/10.1021/acs.chemmater.1c00946
Chem. Mater. 2021, 33, 4541−4550

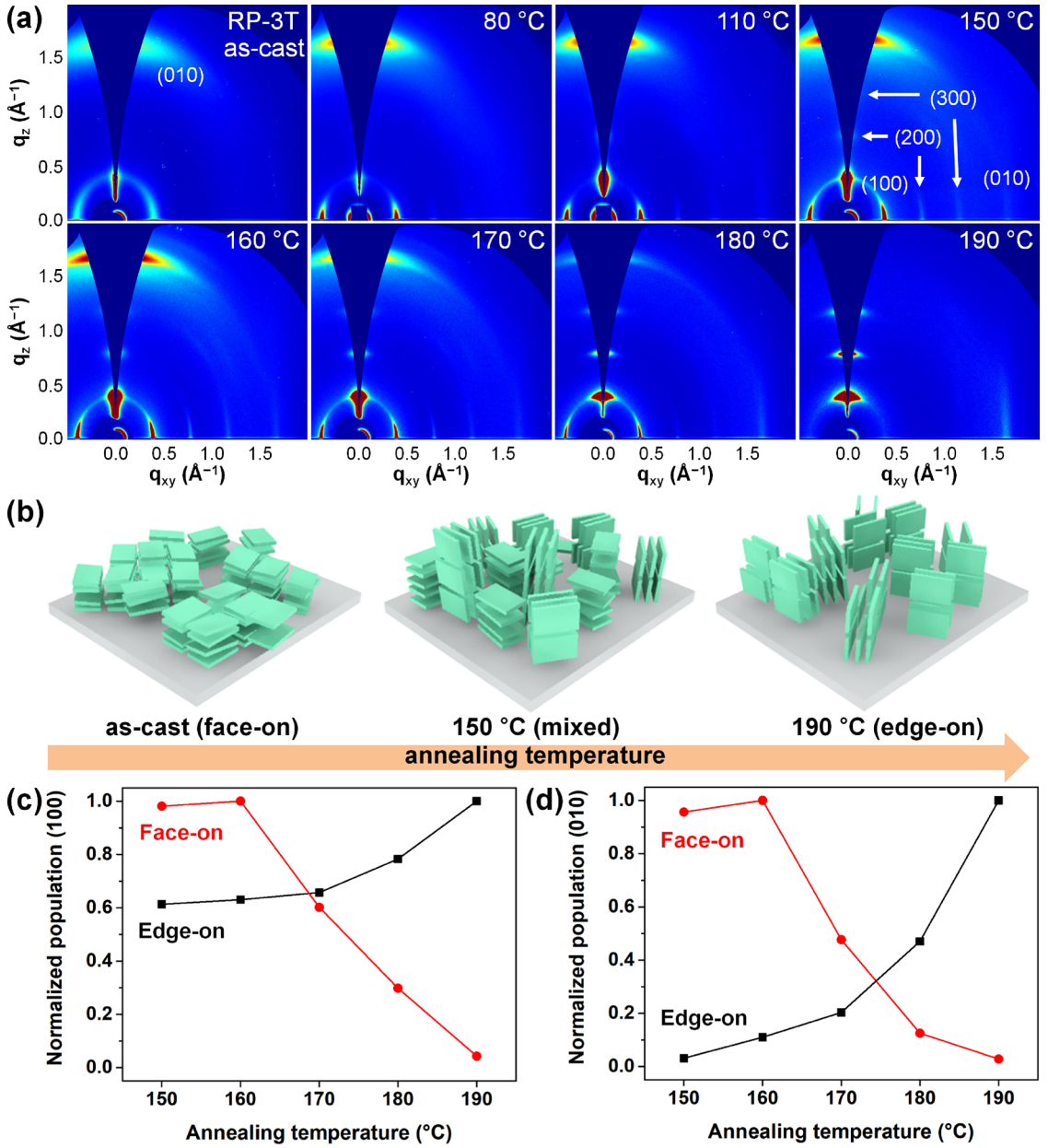

Figure 2. (a) GIWAXS patterns of the RP-3T as-cast film and annealed film at various temperatures. (b) Schematic illustration of the re-orientation of crystallites in RP-3T from predominantly face-on to mixed and then to a predominantly edge-on orientation with increasing annealing temperature. Plots of the normalized population of the crystalline domains with an edge-on or face-on orientation obtained from (c) the lamellar (100) and (d) $\pi-\pi$ stacking (010) peaks from RP-3T annealed films as a function of annealing temperature. The normalized population (100) was obtained by integrating the intensity of the peak (χ = 0−30° in regard to the surface normal for edge-on and χ = 60−90° for face-on) from the geometrically corrected pole figure for the (100) peak shown in Figure S3b and being normalized in regard to the highest value; the normalized population (010) was obtained by integrating the intensity of the peak (χ = 60−90° for edge-on and χ = 0−30° for face-on) from the geometrically corrected pole figure for the (010) peak shown in Figure S3b and being normalized in regard to the highest value. The highest normalized population in the data set was arbitrarily assigned with a value of 1.0.

film starts faintly, showing higher-order (h00) peaks in both out-of-plane and in-plane directions. At 150 °C, the intensity of all peaks becomes even stronger and the in-plane (010) peak starts to appear. These observations indicate the growth of both edge-on and face-on crystallites, resulting in the mixed orientation. The edge-on crystallites likely grew from aggregates with the $\pi-\pi$ stacking direction being parallel to the substrate that were nucleated upon initial spin-coating at room temperature since heterogeneous nucleation occurs more readily than homogeneous nucleation during cold crystallization.[47] However, such aggregates were not shown in the GIWAXS pattern of the as-cast RP-3T film due to lack of long-range order.[48] Further ramping up the annealing temperature, the intensity of out-of-plane (010) and in-plane (h00) peaks starts to weaken at 170 °C and they nearly disappear at 190 °C. In the meantime, the intensity of out-of-plane (h00) and in-plane (010) peaks keeps increasing as the annealing temperature increases to 190 °C. These changes in GIWAXS patterns with increasing annealing temperature clearly show that the re-orientation of crystallites occurs in RP-3T from predominantly face-on to mixed and then to a predominantly edge-on orientation as the annealing temperature increases

https://doi.org/10.1021/acs.chemmater.1c00946
Chem. Mater. 2021, 33, 4541−4550

Table 2. FWHM and q Values of (100) and (010) Peaks in Out-of-Plane and In-Plane Directions in the GIWAXS Patterns of RP-3T Films as a Function of Annealing Temperature[g]

annealing temperature (°C)	out-of-plane direction				in-plane direction			
	(100) peak[a]		(010) peak[b]		(100) peak[c]		(010) peak[d]	
	FWHM (Å^{-1})	q_z (Å^{-1})	FWHM (Å^{-1})	q_z (Å^{-1})	FWHM (Å^{-1})	q_{xy} (Å^{-1})	FWHM (Å^{-1})	q_{xy} (Å^{-1})
no annealing	-[e]	0.409	0.227	1.658	0.070	0.396	-[f]	-[f]
150	0.115	0.401	0.108	1.689	0.024	0.387	-[f]	-[f]
160	0.091	0.401	0.099	1.689	0.021	0.387	-[f]	1.642
170	0.042	0.406	0.092	1.685	0.021	0.387	0.198	1.631
180	0.025	0.406	0.083	1.679	0.020	0.385	0.161	1.622
190	0.023	0.405	-[f]	-[f]	-[f]	0.389	0.122	1.622

[a]Corresponding to the lamellar packing of edge-on crystallites. [b]Corresponding to the $\pi-\pi$ stacking of face-on crystallites. [c]Corresponding to the lamellar packing of face-on crystallites. [d]Corresponding to the $\pi-\pi$ stacking of edge-on crystallites. [e]The corresponding peak is hindered by beam stop shadowing. [f]The corresponding peak is not evident, either too weak or too wide. [g]Edge-on crystallites consist of out-of-plane lamellar packing and in-plane $\pi-\pi$ stacking (shaded), and face-on crystallites consist of in-plane lamellar packing and out-of-plane $\pi-\pi$ stacking (unshaded).

(Figure 2b). It should be noted that the re-orientation of crystallites in RP-3T is already completed before the whole film is melted; by contrast, previously, it was considered that re-orientation possibly occurs due to heterogeneous nucleation of edge-on crystallites at the interface upon cooling from the melt and cannot be achieved upon annealing below the T_m.[31,32]

To investigate the re-orientation behavior of crystallites in RP-3T, we constructed pole figures for the lamellar (100) and $\pi-\pi$ stacking (010) peaks (Figure S3a) and further quantified the relative population of crystallites with a particular orientation χ, the polar angle, for (100) and (010) peaks from RP-3T annealed films (Figure S3b).[49] The relative population of the crystallites was obtained by performing geometrical correction, $\sin(\chi)I(\chi)$, on the pole figures.[10,49] Furthermore, we were able to obtain the normalized population of the crystalline domains with an edge-on or face-on orientation for (100) and (010) peaks separately from RP-3T annealed films as a function of annealing temperature (Figure 2c,d). Specifically, we integrated the intensity of the peak from Figure S3b and normalized the values in regard to the highest value, which was arbitrarily assigned with a value of 1.0. We defined the edge-on crystallites as crystallites with their lamellar stacking direction (100) oriented 0−30° in regard to the surface normal (and 60−90° for face-on crystallites). Similarly, in the case of the $\pi-\pi$ stacking direction (010), we defined the edge-on crystallites as the ones oriented 60−90° to the surface normal (and 0−30° for face-on crystallites) (see Figure S4 for further elaboration).

The normalized population of edge-on crystallites, determined from (100) peaks (Figure 2c) or (010) peaks (Figure 2d), gradually increases with increasing annealing temperature. On the other hand, the normalized population of face-on crystallites, determined from (100) peaks (Figure 2c) or (010) peaks (Figure 2d), starts to decrease at 170 °C and continues the trend to near zero as the annealing temperature increases to 190 °C. These observations confirm that face-on crystallites start to disappear at around 170 °C. We suggest that at elevated temperatures (170 °C and above), face-on crystallites destabilize and the polymer chains most likely enter the surrounding amorphous regions, yet there could be some polymer chains in face-on crystallites that directly add to neighboring edge-on crystallites, i.e., Ostwald ripening. At the same time, edge-on crystallites grow by predominantly consuming amorphous chains until the temperature reaches the T_m.

Furthermore, the full width at half maximum (FWHM) of the out-of-plane (100) and in-plane (010) peaks gradually decreases with increasing annealing temperature (shaded columns in Table 2). This result suggests an increase in coherence length and/or a decrease in paracrystalline disorder in edge-on crystallites.[10] On the other hand, the disappearance of the out-of-plane (010) peak and the drastic weakening and widening of the in-plane (100) peak at 190 °C are indicative of a decrease in the number and the size of face-on crystallites (Figure S5). These observations further support that re-orientation occurs because face-on crystallites disappear, while edge-on crystallites continue to grow as the annealing temperature increases toward the T_m.

We also characterized P3HT films using GIWAXS with increasing annealing temperature to investigate the changes in the orientation of crystallites. As shown in Figure 3, the intensity of out-of-plane (h00) peaks gradually increases with increasing annealing temperature; furthermore, the out-of-plane (010) peak disappears and the arc-shaped (100) scattering peak becomes considerably weakened upon annealing at 220 °C, a temperature slightly below the T_m of P3HT (228 °C). These observations suggest that face-on crystallites in P3HT thin films also disappear before the whole film is melted.

Investigating Re-orientation Mechanisms upon Annealing via NEXAFS. While GIWAXS is mainly sensitive to crystalline domains only, the complementary near-edge X-ray absorption fine structure (NEXAFS) provides information on the average orientation of chains in both crystalline and amorphous domains.[50,51] Specifically, chain orientation can be quantified using the dichroic ratio, $R = (I_{90°} - I_{0°})/(I_{90°} + I_{0°})$, where $I_{90°}$ and $I_{0°}$ are, respectively, the NEXFAS peak intensities at incident angles of 90° and 0°.[51] R can vary from +0.7 to −1, where a more positive R indicates more edge-on orientation, and a more negative R indicates more face-on orientation.[51] We then applied NEXAFS to probe the P3HT and RP-3T films annealed at various temperatures, with the

https://doi.org/10.1021/acs.chemmater.1c00946
Chem. Mater. 2021, 33, 4541−4550

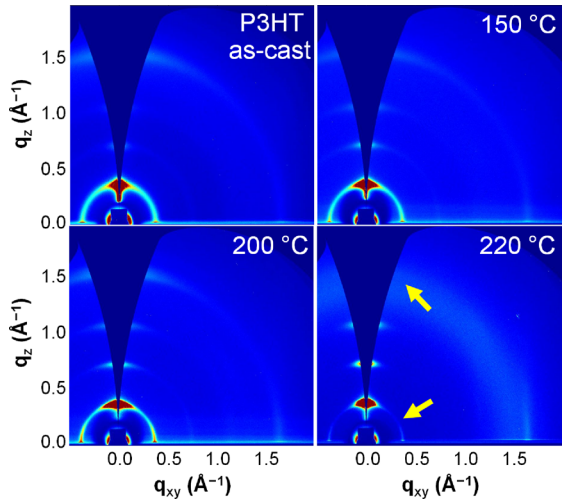

Figure 3. GIWAXS patterns of P3HT as-cast, 150 °C, 200 °C, and 220 °C annealed films. Yellow arrows indicate the disappearance of the out-of-plane (010) peak and weakening of the arc-shaped (100) peak upon annealing at 220 °C.

NEXAFS spectra and *R* values shown in Figure S6 and Table S1, respectively.

As shown in Figure 4, the *R* values of P3HT films annealed at different temperatures are all positive, meaning that the

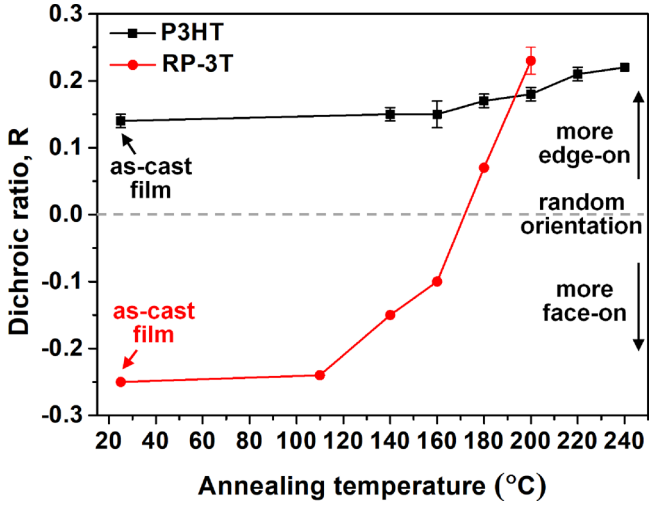

Figure 4. Dichroic ratios of P3HT and RP-3T films measured via NEXAFS spectroscopy as a function of annealing temperature. The annealing temperature of 25 °C means no thermal annealing applied.

average chain orientation in the P3HT films, for both crystalline and amorphous domains, is edge-on over the entire annealing temperature range. As the annealing temperature increases to 240 °C in the case of P3HT, the *R* value increases slightly; this indicates the increase in edge-on orientation character, corroborating the GIWAXS data. In the case of RP-3T, the as-cast film (25 °C) and 110 °C annealed film show similar *R* values around −0.25, which can be attributed to the predominantly face-on orientation of crystallites. As the annealing temperature increases from 110 °C to 160 °C, the *R* value increases (albeit still negative), indicating that there are more amorphous chains that turn into edge-on crystallites than into face-on crystallites, which results in the mixed orientation with the face-on orientation still being dominant. As the annealing temperature further increases from 160 to 180 °C, the *R* value rapidly increases into a positive value; this is likely because face-on crystallites start to disappear in this temperature range, whereas edge-on crystallites continue to grow (Figure 2c,d). The *R* value finally reaches to its highest value as the annealing temperature reaches 200 °C (i.e., melt-annealing), indicating the disappearance of most of face-on crystallites and the sustained growth of edge-on crystallites.

Examining the Impact of Surface and Interface on the Re-orientation. Data from GIWAXS and NEXAFS establish that crystallite re-orientation occurs in RP-3T thin films with increasing annealing temperature toward the T_m. The changes in the microstructures and orientation of crystallites in RP-3T thin films also affect the surface morphologies of the thin films. The surfaces of the as-cast and 140, 170, and 190 °C annealed RP-3T films were probed using atomic force microscopy (AFM) (Figure 5). The as-cast

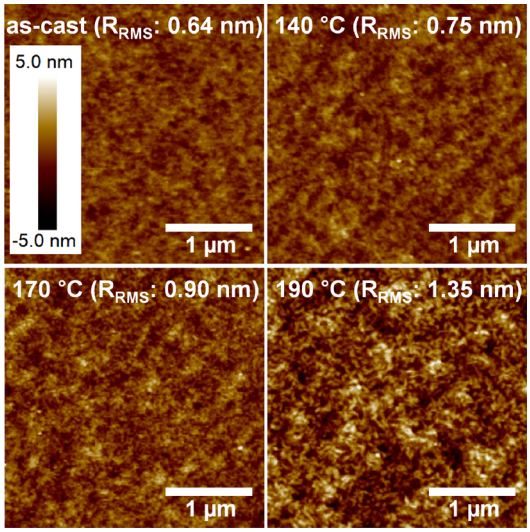

Figure 5. AFM height images of as-cast and 140, 170, and 190 °C annealed films of RP-3T.

film exhibits a root mean squared (RMS) roughness of 0.64 nm. As the annealing temperature increases to 190 °C, the RMS roughness considerably increases to 1.35 nm, which can be attributed to the increasing re-orientation of crystallites from face-on to edge-on and the increase in the coherence length of out-of-plane lamellar packing.[31]

It is generally believed that the kinetically formed texture during the fast spin-coating process can change into another texture with the lowest surface energy upon thermal annealing;[18] furthermore, the earlier study by Zhang et al. on DPP-thiophene copolymers suggested that edge-on orientation is the lowest energy configuration, while face-on orientation is a kinetically trapped metastable state.[14] Thus, it can be inferred that the edge-on crystallites would have a lower surface energy than the face-on crystallites. Applying these assumptions to our case would mean that the surface energy of the RP-3T film would decrease with increasing annealing temperature (since the amount of edge-on crystallites in the RP-3T film increases with increasing annealing temperature). We then measured the surface energy of the as-cast and 140, 170, and 190 °C annealed RP-3T films via contact angle measurement; however, all films exhibited similar surface energies (Figure S7). This result indicates that the difference in surface energy

https://doi.org/10.1021/acs.chemmater.1c00946
Chem. Mater. 2021, 33, 4541−4550

between edge-on and face-on orientations would only play a minor role (if any) in the observed transition from face-on to edge-on upon thermal annealing in the case of RP-3T.

Another factor that is believed to affect molecular packing and orientation is the polymer/substrate interface.[7] To investigate the possible impact of such an interface on the re-orientation observed in the case of RP-3T, we further applied GIWAXS to characterize RP-3T films coated on two additional substrates, bare glass (surface energy of bare glass: 63.9 mJ/m^2)[52] and PEDOT:PSS-coated glass (surface energy of PEDOT:PSS: 71.65−73.43 mJ/m^2);[53] all such films were annealed under the same condition used to prepare otherwise identical films on Si wafers (surface energy of Si wafer: 54.1 mJ/m^2).[54] GIWAXS patterns of these films show a very similar tendency (i.e., face-on crystallites start to disappear at 170 °C, inducing the re-orientation of crystallites from face-on orientation to edge-on orientation) as we observed for RP-3T films on Si wafer (Figure S8). This result suggests that the polymer/substrate interface is not the major factor that induces the re-orientation in RP-3 T.

Implication of the Difference in Packing Distances between Edge-On and Face-On Crystallites. Although the re-orientation of crystallites from face-on to edge-on upon melt-annealing was previously observed in other CPs,[31−35] a unique feature in the case of RP-3T is that the re-orientation is achieved before the whole film is melted. As discussed earlier, this observation suggests that a kinetically trapped metastable state (i.e., face-on orientation) can transition to a more stable state (i.e., edge-on orientation) upon thermal annealing below the T_m. Previously, it has been believed that such transition is driven by lower surface/interface free energies of edge-on crystallites;[31,32] however, we found that surface/interface free energies have a minor impact on the re-orientation in RP-3T. Instead, it is plausible that edge-on crystallites are structurally more stable than face-on crystallites in RP-3T.

We note that most studies on probing crystallite orientation in semicrystalline CPs have not given much attention to the differences in packing distances between edge-on and face-on crystallites. Interestingly, we found that in RP-3T films annealed at any temperature investigated, the lamellar packing distances (d_{100}) in edge-on crystallites are shorter (up to 0.84 Å) than those in face-on crystallites (Figure 6a). Furthermore, $\pi-\pi$ stacking distances (d_{010}) in edge-on crystallites are longer (up to 0.13 Å) than those in face-on crystallites (Figure 6b). These results indicate that the chain packing in RP-3T is tighter along the out-of-plane direction than along the in-plane direction. These differences in packing distances (lamellar and $\pi-\pi$ stacking) between edge-on and face-on crystallites imply that the intermolecular interactions are different in these two types of crystallites, e.g., stronger van der Waals interactions between hexyl side chains (due to the shorter lamellar packing distances up to 0.84 Å) for edge-on crystallites and stronger $\pi-\pi$ stacking interactions between conjugated backbones (due to the shorter $\pi-\pi$ stacking distances up to 0.13 Å) for face-on crystallites. Considering that face-on orientation is a kinetically trapped metastable state, while edge-on orientation is a more stable state, we speculate that stronger van der Waals interactions between hexyl side chains in edge-on crystallites would play a more important role in determining the stability of crystallites than stronger $\pi-\pi$ stacking interactions between conjugated backbones in face-on crystallites in RP-3T. Although we do not currently understand the underlying reason for the different packing distances between edge-on and face-on crystallites in RP-3T, it should be noted that our P3HT and other CPs that show the re-orientation of crystallites from face-on to edge-on upon melt-annealing also exhibit tighter packing distances along the out-of-plane direction than those along the in-plane direction.[31−33] More simulation/experimental works are required to further explain the difference in packing distance and its implications.

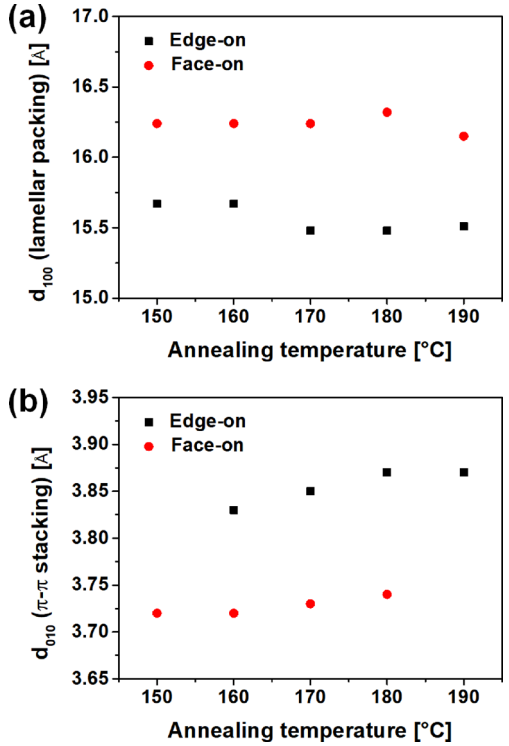

Figure 6. Plots of (a) d_{100} (lamellar packing) and (b) d_{010} ($\pi-\pi$ stacking) as a function of annealing temperature for edge-on and face-on crystallites in P3HT.

CONCLUSIONS

The copolymer RP-3T, where unsubstituted terthiophene (3T) units are inserted into the regioregular P3HT in a random manner, offered a model system to investigate the re-orientation of crystallites from face-on to edge-on upon melt-annealing, an intriguing phenomenon that has been previously shown in a number of CPs. The accumulated data with RP-3T suggest a complete picture as follows. The initial dominating face-on crystallites in the as-cast film grow with the annealing temperature until ∼170 °C, at which the face-on crystallites begin to disappear and the polymer chain would enter the surrounding amorphous region or migrate to edge-on crystallites. In the meantime, the edge-on crystallites also grow in the entire annealing temperature range. As the annealing temperature increases further to 190 °C, most of face-on crystallites disappear and the only remaining crystallites are edge-on. Thus, this picture offers a reasonable mechanism on how a thin film morphology with preferential face-on orientation transitions to predominantly edge-on orientation as the annealing temperature increases toward the T_m. Furthermore, our study reveals that edge-on crystallites have shorter lamellar packing distances than face-on crystallites, which could lead to the more stable edge-on crystallites and, hence, the re-orientation. Nevertheless, further study is needed to address another fundamental question: why

https://doi.org/10.1021/acs.chemmater.1c00946
Chem. Mater. 2021, 33, 4541−4550

the chain packing is tighter along the out-of-plane direction than along the in-plane direction. Finally, we want to emphasize that our interpretation, based on obtained experimental data, could only apply to systems where similar experimental data are observed.

EXPERIMENTAL SECTION

General Experimental Details. All chemicals were purchased from commercial sources (Sigma-Aldrich, Fisher, Acros, etc.) and were used as received except when specified. Anhydrous THF was prepared using a J.C. Meyer solvent dispensing system. The specific synthetic procedure is shown in the Supporting Information. ^{1}H nuclear magnetic resonance (NMR) measurements were recorded with a Bruker DPX spectrometer (500 MHz) FT NMR system. Molecular weights were determined by size exclusion chromatography with SHIMADZU LC solution with chlorobenzene eluent at a flow rate of 1.0 mL/min. Molecular weight and dispersity data are reported relative to 580−200,000 g/mol poly(styrene) standards. Differential scanning calorimetric (DSC) measurements were performed using a PerkinElmer Pyris 1 DSC instrument under a N_2 atmosphere at a heating and cooling rate of 10 °C/min. The surface morphology was scanned by an atomic force microscope of VEECO Dimension 3100 equipped with Nanoscope V (ver. 7.0). The film thicknesses were recorded by a profilometer (Alpha-Step 200, Tencor Instruments).

Film Preparation (on the Si or Glass Substrate). P3HT and RP-3T solutions (5 mg/mL) in chloroform were prepared. Si or glass substrates were rinsed with deionized water, acetone, and isopropyl alcohol, followed by a 15 min UV-ozone treatment. The polymer solutions were spin-coated on a substrate at 500 rpm for 60 s to give a thin film with a thickness of 60 to 70 nm. The films were annealed at a predetermined temperature for 10 min and cooled back to room temperature under an ambient condition.

Film Preparation (on the PEDOT:PSS/Glass Substrate). An RP-3T solution (5 mg/mL) in chloroform was prepared. Glass substrates were rinsed with deionized water, acetone, and isopropyl alcohol, followed by a 15 min UV-ozone treatment. PEDOT:PSS (20 mg/mL) in deionized water was spin-coated on a glass substrate at 3000 rpm for 30 s, followed by thermal annealing at 140 °C for 10 min. Then, the polymer solutions were spin-coated on a PEDOT:PSS-coated substrate at 500 rpm for 60 s. The films were annealed at a predetermined temperature for 10 min and cooled back to room temperature under an ambient condition.

Grazing Incidence Wide-Angle X-ray Scattering (GIWAXS) Measurements. GIWAXS experiments were carried out with a sample-to-detector distance of 212 mm and an X-ray radiation beam energy of 10.26 keV. The incidence angle for the X-ray beam was set to 0.12°. The diffraction patterns were collected with a Rayonix 2D MAR165 image plate. The GIWAXS measurements were carried out in a vacuum chamber.

Near-Edge X-ray Absorption Fine Structure (NEXAFS). Carbon K-edge (C1s) collection was performed in total-electron-yield mode with a beam energy of 350 eV. The spectra were collected at four incidence angles with respect to the surface plane (30°, 45°, 55°, and 70°). The C1s NEXAFS raw data were normalized with respect to the carbon concentration by their intensity at 324 eV.

ASSOCIATED CONTENT

Supporting Information

The Supporting Information is available free of charge at https://pubs.acs.org/doi/10.1021/acs.chemmater.1c00946.

Detailed synthetic procedures; ^{1}H NMR spectra; pole figures and relative population data; illustrations of extracting GIWAXS peak intensity; GIWAXS and NEXAFS spectra; contact angle data; dichroic ratios; information on packing distances (PDF)

AUTHOR INFORMATION

Corresponding Authors

Taiho Park − *Department of Chemical Engineering, Pohang University of Science and Technology (POSTECH), Pohang, Gyeongbuk 37673, Korea;* orcid.org/0000-0002-5867-4679; Email: taihopark@postech.ac.kr

Wei You − *Department of Chemistry, University of North Carolina at Chapel Hill, Chapel Hill, North Carolina 27599, United States;* orcid.org/0000-0003-0354-1948; Email: wyou@unc.edu

Author

Sung Yun Son − *Department of Chemical Engineering, Pohang University of Science and Technology (POSTECH), Pohang, Gyeongbuk 37673, Korea; Department of Chemistry, University of North Carolina at Chapel Hill, Chapel Hill, North Carolina 27599, United States;* orcid.org/0000-0003-1563-5474

Complete contact information is available at: https://pubs.acs.org/10.1021/acs.chemmater.1c00946

Author Contributions

The manuscript was written through contributions of all authors.

Notes

The authors declare no competing financial interest.

ACKNOWLEDGMENTS

GIWAXS and NEXAFS measurements were performed at a synchrotron radiation facility on the beamlines 3C and 4D, respectively, at Pohang Accelerator Laboratory (PAL), Korea. This work was supported by NSF (award CBET-1639429 for S.Y.S. and W.Y.) and National Research Foundation of Korea (NRF) funded by the Korea government (MSIT) (No. 2021R1A2C3004420, for T.P).

REFERENCES

(1) Beaujuge, P. M.; Fréchet, J. M. J. Molecular design and ordering effects in π-functional materials for transistor and solar cell applications. *J. Am. Chem. Soc.* **2011**, *133*, 20009.

(2) Ong, B. S.; Wu, Y.; Liu, P.; Gardner, S. High-performance semiconducting polythiophenes for organic thin-film transistors. *J. Am. Chem. Soc.* **2004**, *126*, 3378.

(3) Yan, H.; Chen, Z.; Zheng, Y.; Newman, C.; Quinn, J. R.; Dotz, F.; Kastler, M.; Facchetti, A. A high-mobility electron-transporting polymer for printed transistors. *Nature* **2009**, *457*, 679.

(4) Price, S. C.; Stuart, A. C.; Yang, L.; Zhou, H.; You, W. Fluorine substituted conjugated polymer of medium band gap yields 7% efficiency in polymer−fullerene solar cells. *J. Am. Chem. Soc.* **2011**, *133*, 4625.

(5) Zhou, H.; Yang, L.; You, W. Rational design of high performance conjugated polymers for organic solar cells. *Macromolecules* **2012**, *45*, 607.

(6) Sirringhaus, H. 25th anniversary article: organic field-effect transistors: the path beyond amorphous silicon. *Adv. Mater.* **2014**, *26*, 1319.

(7) Kline, R. J.; McGehee, M. D.; Toney, M. F. Highly oriented crystals at the buried interface in polythiophene thin-film transistors. *Nat. Mater.* **2006**, *5*, 222.

(8) Noriega, R.; Rivnay, J.; Vandewal, K.; Koch, F. P. V.; Stingelin, N.; Smith, P.; Toney, M. F.; Salleo, A. A general relationship between disorder, aggregation and charge transport in conjugated polymers. *Nat. Mater.* **2013**, *12*, 1038.

(9) Tumbleston, J. R.; Collins, B. A.; Yang, L.; Stuart, A. C.; Gann, E.; Ma, W.; You, W.; Ade, H. The influence of molecular orientation on organic bulk heterojunction solar cells. *Nat. Photon.* **2014**, *8*, 385.
(10) Rivnay, J.; Mannsfeld, S. C. B.; Miller, C. E.; Salleo, A.; Toney, M. F. Quantitative determination of organic semiconductor microstructure from the molecular to device scale. *Chem. Rev.* **2012**, *112*, 5488.
(11) Sirringhaus, H.; Brown, P.; Friend, R.; Nielsen, M. M.; Bechgaard, K.; Langeveld-Voss, B.; Spiering, A.; Janssen, R. A.; Meijer, E.; Herwig, P.; de Leeuw, D. M. Two-dimensional charge transport in self-organized, high-mobility conjugated polymers. *Nature* **1999**, *401*, 685.
(12) Salleo, A. Charge transport in polymeric transistors. *Mater. Today* **2007**, *10*, 38.
(13) Tsao, H. N.; Müllen, K. Improving polymer transistor performance via morphology control. *Chem. Soc. Rev.* **2010**, *39*, 2372.
(14) Zhang, X.; Richter, L. J.; DeLongchamp, D. M.; Kline, R. J.; Hammond, M. R.; McCulloch, I.; Heeney, M.; Ashraf, R. S.; Smith, J. N.; Anthopoulos, T. D.; Schroeder, B.; Geerts, Y. H.; Fischer, D. A.; Toney, M. F. Molecular packing of high-mobility diketo pyrrolopyrrole polymer semiconductors with branched alkyl side chains. *J. Am. Chem. Soc.* **2011**, *133*, 15073.
(15) Kim, Y.; Long, D. X.; Lee, J.; Kim, G.; Shin, T. J.; Nam, K.-W.; Noh, Y.-Y.; Yang, C. A balanced face-on to edge-on texture ratio in naphthalene diimide-based polymers with hybrid siloxane chains directs highly efficient electron transport. *Macromolecules* **2015**, *48*, 5179.
(16) Chen, M. S.; Niskala, J. R.; Unruh, D. A.; Chu, C. K.; Lee, O. P.; Fréchet, J. M. J. Control of polymer-packing orientation in thin films through synthetic tailoring of backbone coplanarity. *Chem. Mater.* **2013**, *25*, 4088.
(17) Mueller, C. J.; Gann, E.; Singh, C. R.; Thelakkat, M.; McNeill, C. R. Control of molecular orientation in polydiketopyrrolopyrrole copolymers via diffusive noncovalent interactions. *Chem. Mater.* **2016**, *28*, 7088.
(18) Kim, H. G.; Kang, B.; Ko, H.; Lee, J.; Shin, J.; Cho, K. Synthetic tailoring of solid-state order in diketopyrrolopyrrole-based copolymers via intramolecular noncovalent interactions. *Chem. Mater.* **2015**, *27*, 829.
(19) Chen, M. S.; Lee, O. P.; Niskala, J. R.; Yiu, A. T.; Tassone, C. J.; Schmidt, K.; Beaujuge, P. M.; Onishi, S. S.; Toney, M. F.; Zettl, A.; Fréchet, J. M. J. Enhanced solid-state order and field-effect hole mobility through control of nanoscale polymer aggregation. *J. Am. Chem. Soc.* **2013**, *135*, 19229.
(20) Mei, J.; Kim, D. H.; Ayzner, A. L.; Toney, M. F.; Bao, Z. Siloxane-terminated solubilizing side chains: bringing conjugated polymer backbones closer and boosting hole mobilities in thin-film transistors. *J. Am. Chem. Soc.* **2011**, *133*, 20130.
(21) Lee, J.; Han, A.-R.; Yu, H.; Shin, T. J.; Yang, C.; Oh, J. H. Boosting the ambipolar performance of solution-processable polymer semiconductors via hybrid side-chain engineering. *J. Am. Chem. Soc.* **2013**, *135*, 9540.
(22) Chang, J.-F.; Sun, B.; Breiby, D. W.; Nielsen, M. M.; Sölling, T. I.; Giles, M.; McCulloch, I.; Sirringhaus, H. Enhanced mobility of poly (3-hexylthiophene) transistors by spin-coating from high-boiling-point solvents. *Chem. Mater.* **2004**, *16*, 4772.
(23) Kitchen, B.; Awartani, O.; Kline, R. J.; McAfee, T.; Ade, H.; O'Connor, B. T. Tuning Open-Circuit Voltage in Organic Solar Cells with Molecular Orientation. *ACS Appl. Mater. Interfaces* **2015**, *7*, 13208.
(24) DeLongchamp, D. M.; Vogel, B. M.; Jung, Y.; Gurau, M. C.; Richter, C. A.; Kirillov, O. A.; Obrzut, J.; Fischer, D. A.; Sambasivan, S.; Richter, L. J.; Lin, E. K. Variations in semiconducting polymer microstructure and hole mobility with spin-coating speed. *Chem. Mater.* **2005**, *17*, 5610.
(25) Aasmundtveit, K.; Samuelsen, E.; Guldstein, M.; Steinsland, C.; Flornes, O.; Fagermo, C.; Seeberg, T.; Pettersson, L.; Inganäs, O.; Feidenhans'l, R.; Ferrer, S. Structural anisotropy of poly (alkylthiophene) films. *Macromolecules* **2000**, *33*, 3120.
(26) Schott, S.; Gann, E.; Thomsen, L.; Jung, S. H.; Lee, J. K.; McNeill, C. R.; Sirringhaus, H. Charge-transport anisotropy in a uniaxially aligned diketopyrrolopyrrole-based copolymer. *Adv. Mater.* **2015**, *27*, 7356.
(27) Gargi, D.; Kline, R. J.; DeLongchamp, D. M.; Fischer, D. A.; Toney, M. F.; O'Connor, B. T. Charge transport in highly face-on poly (3-hexylthiophene) films. *J. Phys. Chem. C* **2013**, *117*, 17421.
(28) Kim, D. H.; Park, Y. D.; Jang, Y.; Yang, H.; Kim, Y. H.; Han, J. I.; Moon, D. G.; Park, S.; Chang, T.; Chang, C.; Joo, M.; Ryu, C. Y.; Cho, K. Enhancement of Field-Effect Mobility Due to Surface-Mediated Molecular Ordering in Regioregular Polythiophene Thin Film Transistors. *Adv. Funct. Mater.* **2005**, *15*, 77.
(29) Brinkmann, M.; Gonthier, E.; Bogen, S.; Tremel, K.; Ludwigs, S.; Hufnagel, M.; Sommer, M. Segregated versus mixed interchain stacking in highly oriented films of naphthalene diimide bithiophene copolymers. *ACS Nano* **2012**, *6*, 10319.
(30) Kim, D. H.; Jang, Y.; Park, Y. D.; Cho, K. Layered Molecular Ordering of Self-Organized Poly(3-hexylthiophene) Thin Films on Hydrophobized Surfaces. *Macromolecules* **2006**, *39*, 5843.
(31) Verploegen, E.; Mondal, R.; Bettinger, C. J.; Sok, S.; Toney, M. F.; Bao, Z. Effects of Thermal Annealing Upon the Morphology of Polymer-Fullerene Blends. *Adv. Funct. Mater.* **2010**, *20*, 3519.
(32) Rivnay, J.; Steyrleuthner, R.; Jimison, L. H.; Casadei, A.; Chen, Z.; Toney, M. F.; Facchetti, A.; Neher, D.; Salleo, A. Drastic Control of Texture in a High Performance n-Type Polymeric Semiconductor and Implications for Charge Transport. *Macromolecules* **2011**, *44*, 5246.
(33) Son, S. Y.; Lee, G. Y.; Kim, S.; Park, W. T.; Park, S. A.; Noh, Y. Y.; Park, T. Control of Crystallite Orientation in Diketopyrrolopyrrole-Based Semiconducting Polymers via Tuning of Intermolecular Interactions. *ACS Appl. Mater. Interfaces* **2019**, *11*, 10751.
(34) Yang, H.; Wang, L.; Zhang, J.; Yu, X.; Geng, Y.; Han, Y. Molecular Packing and Orientation Transition of Crystalline Poly (2, 5-dihexyloxy-p-phenylene). *Macromol. Chem. Phys.* **2014**, *215*, 405.
(35) Yang, H.; Zhang, R.; Wang, L.; Zhang, J.; Yu, X.; Liu, J.; Xing, R.; Geng, Y.; Han, Y. Face-on and Edge-on Orientation Transition and Self-Epitaxial Crystallization of All-Conjugated Diblock Copolymer. *Macromolecules* **2015**, *48*, 7557.
(36) Seifrid, M. T.; Oosterhout, S. D.; Toney, M. F.; Bazan, G. C. Kinetic Versus Thermodynamic Orientational Preferences for a Series of Isomorphic Molecular Semiconductors. *ACS Omega* **2018**, *3*, 10198.
(37) Tremel, K.; Fischer, F. S. U.; Kayunkid, N.; Pietro, R. D.; Tkachov, R.; Kiriy, A.; Neher, D.; Ludwigs, S.; Brinkmann, M. Charge Transport Anisotropy in Highly Oriented Thin Films of the Acceptor Polymer P(NDI2OD-T2). *Adv. Energy Mater.* **2014**, *4*, 1301659.
(38) Kim, Y.; Cook, S.; Tuladhar, S. M.; Choulis, S. A.; Nelson, J.; Durrant, J. R.; Bradley, D. D. C.; Giles, M.; McCulloch, I.; Ha, C.-S.; Ree, M. A strong regioregularity effect in self-organizing conjugated polymer films and high-efficiency polythiophene: fullerene solar cells. *Nat. Mater.* **2006**, *5*, 197.
(39) Kline, R. J.; McGehee, M. D.; Kadnikova, E. N.; Liu, J.; Fréchet, J. M. J. Controlling the field-effect mobility of regioregular polythiophene by changing the molecular weight. *Adv. Mater.* **2003**, *15*, 1519.
(40) Kim, J.-S.; Kim, J.-H.; Lee, W.; Yu, H.; Kim, H. J.; Song, I.; Shin, M.; Oh, J. H.; Jeong, U.; Kim, T.-S.; Kim, B. J. Tuning mechanical and optoelectrical properties of poly (3-hexylthiophene) through systematic regioregularity control. *Macromolecules* **2015**, *48*, 4339.
(41) Iovu, M. C.; Sheina, E. E.; Gil, R. R.; McCullough, R. D. Experimental evidence for the quasi-"living" nature of the grignard metathesis method for the synthesis of regioregular poly (3-alkylthiophenes). *Macromolecules* **2005**, *38*, 8649.
(42) Miyakoshi, R.; Yokoyama, A.; Yokozawa, T. Catalyst-transfer polycondensation. Mechanism of Ni-catalyzed chain-growth polymerization leading to well-defined poly (3-hexylthiophene). *J. Am. Chem. Soc.* **2005**, *127*, 17542.

https://doi.org/10.1021/acs.chemmater.1c00946
Chem. Mater. 2021, 33, 4541−4550

(43) Son, S. Y.; Kim, Y.; Lee, J.; Lee, G.-Y.; Park, W.-T.; Noh, Y.-Y.; Park, C. E.; Park, T. High-field-effect mobility of low-crystallinity conjugated polymers with localized aggregates. *J. Am. Chem. Soc.* **2016**, *138*, 8096.
(44) Trznadel, M.; Pron, A.; Zagorska, M.; Chrzaszcz, R.; Pielichowski, J. Effect of molecular weight on spectroscopic and spectroelectrochemical properties of regioregular poly (3-hexylthiophene). *Macromolecules* **1998**, *31*, 5051.
(45) Son, S. Y.; Kim, J. W.; Lee, J.; Kim, G.-W.; Hong, J.; Kim, J. Y.; Park, T. A donor−acceptor semiconducting polymer with a random configuration for efficient, green-solvent-processable flexible solar cells. *J. Mater. Chem. A* **2018**, *6*, 24580.
(46) Son, S. Y.; Kim, J.-H.; Song, E.; Choi, K.; Lee, J.; Cho, K.; Kim, T.-S.; Park, T. Exploiting $\pi-\pi$ stacking for stretchable semiconducting polymers. *Macromolecules* **2018**, *51*, 2572.
(47) Furushima, Y.; Schick, C.; Toda, A. Crystallization, recrystallization, and melting of polymer crystals on heating and cooling examined with fast scanning calorimetry. *Polym. Cryst.* **2018**, *1*, No. e10005.
(48) Duong, D. T.; Toney, M. F.; Salleo, A. Role of confinement and aggregation in charge transport in semicrystalline polythiophene thin films. *Phys. Rev. B* **2012**, *86*, 205205.
(49) Diao, Y.; Zhou, Y.; Kurosawa, T.; Shaw, L.; Wang, C.; Park, S.; Guo, Y.; Reinspach, J. A.; Gu, K.; Gu, X.; Tee, B. C. K.; Pang, C.; Yan, H.; Zhao, D.; Toney, M. F.; Mannsfeld, S. C. B.; Bao, Z. Flow-enhanced solution printing of all-polymer solar cells. *Nat. Commun.* **2015**, *6*, 7955.
(50) DeLongchamp, D. M.; Sambasivan, S.; Fischer, D. A.; Lin, E. K.; Chang, P.; Murphy, A. R.; Fréchet, J. M. J.; Subramanian, V. Direct correlation of organic semiconductor film structure to field-effect mobility. *Adv. Mater.* **2005**, *17*, 2340.
(51) DeLongchamp, D. M.; Kline, R. J.; Fischer, D. A.; Richter, L. J.; Toney, M. F. Molecular characterization of organic electronic films. *Adv. Mater.* **2011**, *23*, 319.
(52) Weng, S.-C.; Fuh, A. Y.-G.; Tang, F.-C.; Cheng, K.-T. Effect of surface condition on liquid crystal photoalignment by light-induced azo dye adsorption phenomena. *Liq. Cryst.* **2016**, *43*, 1221−1229.
(53) Petrosino, M.; Rubino, A. The effect of the PEDOT: PSS surface energy on the interface potential barrier. *Synth. Met.* **2012**, *161*, 2714−2717.
(54) Di, C.-a.; Yu, G.; Liu, Y.; Guo, Y.; Sun, X.; Zheng, J.; Wen, Y.; Wang, Y.; Wu, W.; Zhu, D. Effect of dielectric layers on device stability of pentacene-based field-effect transistors. *Phys. Chem. Chem. Phys.* **2009**, *11*, 7268−7273.

https://doi.org/10.1021/acs.chemmater.1c00946
Chem. Mater. 2021, 33, 4541−4550